

Poisson's ratio and the fragility of glass-forming liquids

V. N. Novikov^{1,2} & A. P. Sokolov¹

¹Department of Polymer Science, The University of Akron, Akron, Ohio 44325-3909, USA

²IA&E, Russian Academy of Sciences, Novosibirsk 630090, Russia

The nature of the transformation by which a supercooled liquid 'freezes' to a glass—the glass transition—is a central issue in condensed matter physics^{1–3} but also affects many other fields, including biology⁴. Substantial progress has been made in understanding this phenomenon over the past two decades, yet many key questions remain. In particular, the factors that control the temperature-dependent relaxation and viscous properties of the liquid phase as the glass transition is approached (that is, whether the glass-forming liquid is 'fragile' or 'strong'^{5–7}) remain unclear. Here we show that the fragility of a glass-forming liquid is intimately linked to a very basic property of the corresponding glass phase: the relative strength of shear and bulk moduli, or Poisson's ratio.

Fragility of liquids is defined as the apparent activation energy of shear viscosity η or structural relaxation time τ_α at the glass transition temperature T_g , normalized to T_g (ref. 7):

$$m = \left. \frac{\partial \log \eta(T)}{\partial (T_g/T)} \right|_{T=T_g} \quad (1)$$

It characterizes the steepness of the slope of $\log \eta$ dependence on T_g/T near T_g (Fig. 1). A stronger deviation from Arrhenius behaviour corresponds to a more fragile system. One of the puzzles that remains unsolved is the correlation of the fast terahertz dynamics and fragility^{8,9}: one can predict fragility, that is, temperature variations of τ_α or η in a supercooled liquid at $T \approx T_g$, from analysis of vibrational spectra at terahertz frequencies deep in the glassy state ($T \ll T_g$)^{8,9}. Interest in this puzzle was recently stimulated by ref. 9 (see also refs 10 and 11). Our present goal is to gain better insight into fragility on the microscopic scale and to suggest a consistent explanation for these correlations.

It is well understood that the glass transition is a failure of the material to support shear stress on the typical laboratory timescale of, say, a few minutes. So, shear modulus G is apparently an important parameter. To be more precise, the modulus is frequency-dependent and one needs to consider G at frequencies much higher than the inverse structural relaxation time, that is, the so-called instantaneous shear modulus G_∞ . In an isotropic solid like glass there is only one different independent elastic constant that makes it possible to get the dimensionless parameter proportional to G_∞ , namely, the instantaneous bulk modulus K_∞ . The ratio of instantaneous shear and bulk moduli can be estimated from the ratio of longitudinal ($v_l^2 = M_\infty/\rho$) and transverse ($v_t^2 = G_\infty/\rho$) sound velocities in the glassy state, for example, $K_\infty/G_\infty \propto (v_l/v_t)^2 - 4/3$ (here ρ is the mass density and $M_\infty = K_\infty + (4/3)G_\infty$ is the instantaneous longitudinal modulus). We note that the high-frequency sound velocity in glasses is connected with the adiabatic bulk modulus, although the difference between the isothermal and adiabatic bulk moduli in the glassy state is very small. Analysis of a large number of glasses, including covalent and hydrogen-bonded, van-der-Waals and ionic glasses, shows a correlation between v_l/v_t and m (Fig. 2): the more weakly the system resists the shear stress in comparison with the bulk one in the glassy state (higher v_l/v_t), the more fragile its behaviour appears in the melt. We emphasize that the data presented in Fig. 2 includes all the systems we were able to find in the literature, excluding polymers. It is known that the

fragility of some polymers strongly depends on molecular weight, M_w (ref. 12). For example, the fragility of polystyrene varies from 60 at low M_w up to 150 at high M_w (ref. 12), and only low- M_w polystyrene is in agreement with the correlation of Fig. 2. This sharp increase in fragility with M_w might be polymer-specific; for this reason, all polymers were excluded from consideration, although low fragility polymers like polyisobutylene and polybutadiene agree well with the correlation of Fig. 2.

The inset in Fig. 2 shows the correlation of fragility m with K_∞/G_∞ of the respective glass; it can be well described by the relationship:

$$m - 17 = 29(K_\infty/G_\infty - 1) \text{ or } m = 29(K_\infty/G_\infty - 0.41) \quad (2)$$

where 17 is the lowest value expected for m and K_∞/G_∞ in glasses is not expected to be lower than 1 (for strong glasses like silica and BeF₂, $K_\infty/G_\infty \approx 1.1$). We note that correlation (equation (2)) means also that fragility of a liquid is fully determined just by the Poisson ratio of its glass.

How can one explain the correlation between the fragility of a liquid and the ratio of the instantaneous elastic moduli of a glass (Fig. 2)? The answer might be buried deep in the liquid state because the structure and properties of a glass are essentially the structure and properties of a 'frozen' liquid. Owing to the construction of the fragility plot, all viscosity or relaxation time curves intersect at two points: (1) at T_g , $\log \eta \equiv \log \eta_g = 13$ (where η is in poise), or $\log \tau_\alpha \approx 3$ (where τ is in seconds); and (2) at very high temperatures, $T_g/T \rightarrow 0$, where all liquids have $\log \eta \equiv \log \eta_0 \approx -4$ (ref. 13) or $\log \tau_\alpha \approx \log \tau_0 \approx -14$. This means that if a liquid has a steeper slope of $\log \eta$ near T_g , it inevitably has a smaller slope of $\log \eta$ at high temperature. At high temperatures, relaxation in most of the liquids shows Arrhenius temperature dependence: $\eta = \eta_0 \exp(E/T)$. Thus the high-temperature slope of $\log \eta$ in Fig. 1, E/T_g , can also be a measure of fragility. Experimental data show that E/T_g indeed correlates with fragility m (Fig. 3):

$$\frac{E}{T_g} = \frac{(19.2)^2 \ln 10}{m} \quad (3)$$

We note that a similar relationship with a slightly different coefficient $(17)^2 \ln 10$ follows from the Vogel–Fulcher–Tamman (VFT) equation, $\eta = \eta_0 \exp B/(T - T_0)$, if one assumes that the VFT equation is valid over the entire temperature range. The quantitative disagreement can be related to the well-known fact that a single VFT equation cannot accurately describe η at all temperatures¹⁴.

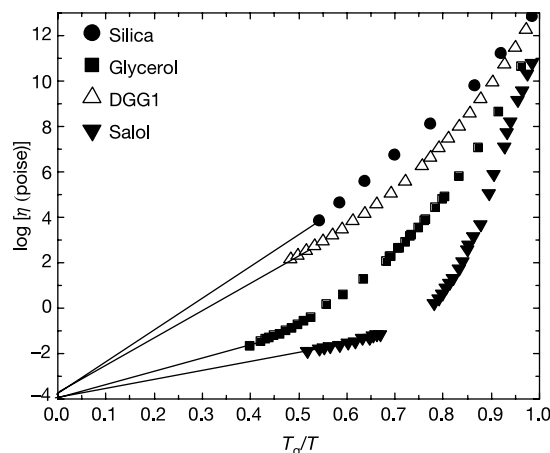


Figure 1 An example of a fragility plot. Data is from refs 2, 27 and 28. DGG1 is a soda-lime silica glass; see Supplementary Table 1. The solid lines show the expected high-temperature slopes E/T_g .

This connection between m and T_g/E helps to explain the correlation between m and the ratio of instantaneous elastic moduli in the glassy state, equation (2). Various authors^{6,15,16} suggest that the activation energy of viscosity is proportional to the instantaneous shear modulus G_∞ , that is, $E \propto G_\infty V_c$, where V_c is some volume that does not show significant temperature variations at high T . On the other hand, there are empirical correlations between elastic moduli of a glass and T_g (for example, refs 6, 17 and 18). However, it is not obvious which combination of shear and bulk moduli is important because these correlations were usually considered within a class of materials with similar chemical structure, and thus with a similar Poisson's ratio. We note that the free volume model for the glass transition¹⁸ predicts $T_g \propto K_\infty$. Analysis of experimental data reveals correlation of T_g/E to the same parameter ($K_\infty/G_\infty - 0.41$) as in equation (2):

$$T_g/E \approx 0.037(K_\infty/G_\infty - 0.41) \propto m \quad (4)$$

Thus, the correlation found (equations (2) or (4) and Fig. 2) emphasizes a very simple rule: the better the glass can resist shear deformation rather than dilatation, the stronger (that is, more Arrhenius-like) the behaviour that is exhibited during its structural relaxation.

On a timescale longer than that of structural relaxation, $t \gg \tau_\alpha$, the shear modulus (for non-polymeric systems) relaxes to zero while the longitudinal modulus relaxes to some finite value M_0 . This leads to a difference between instantaneous (v_∞) and zero-frequency (v_0) longitudinal sound velocities in glasses. The difference provides an estimate of the relaxation strength of the α -process, that is, the so-called non-ergodicity parameter, $f_0 = 1 - v_0^2/v_\infty^2$. A sizeable part of the decrease of the longitudinal sound velocity at $\omega\tau_\alpha \ll 1$ is due to relaxation of the shear modulus. Because $M = K + (4/3)G$, a crude approximation then gives:

$$f_0 \approx (4/3)v_t^2/v_l^2 = G_\infty/[3/4K_\infty + G_\infty] \quad (5)$$

Thus, the ratio G_∞/K_∞ also determines the amplitude of the non-ergodicity parameter.

Equations (5) and (4) lead us directly to an explanation of the

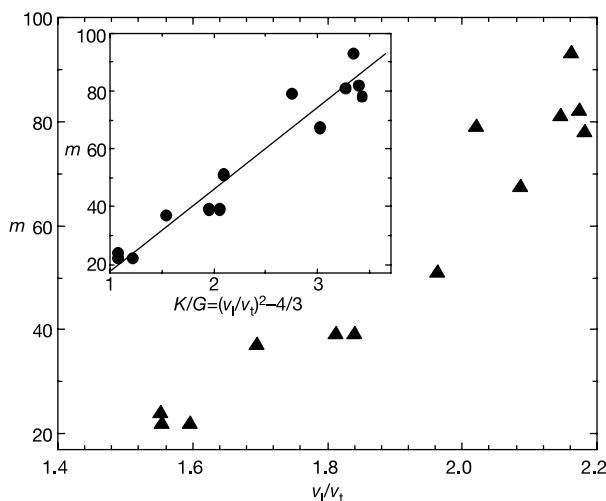


Figure 2 Correlation between fragility and the ratio of longitudinal and transversal sound velocities found in the glassy state. Inset, correlation of fragility with the ratio of the bulk and shear moduli in the glassy state. The straight line shows the relationship from equation (2). Materials (in descending order of fragility): KKN ($\text{Ca}_2(\text{NO}_3)_2\text{-KNO}_3$), m-TCP (m-tricresyl phosphate), OTP (o-therphenyl), Se, m-toluidine, salol, glycerol, B_2O_3 , As_2S_3 , $20(\text{Na}_2\text{O})80(\text{SiO}_2)$, SiO_2 , GeO_2 , BeF_2 . In those cases where more than one value of fragility is known, we used the average value. Data from the literature for fragility, v_t and v_l and the respective references are given in Supplementary Table 1.

recent puzzling observation reported in ref. 9. The authors found that the parameter α , defined as $\alpha = R_{\text{LP}}^{-1}(T)T_g/T$, measured using inelastic X-ray scattering in a few glasses, correlates with their fragility, $\alpha \propto m$. (Here $R_{\text{LP}}(T) = I_c/2I_{\text{Br}}$ is the Landau–Placzek ratio, and $2I_{\text{Br}}$ and I_c are the integrated intensities of the combined Brillouin doublet and the central line of the dynamic structure factor $S(q,\omega)$, respectively.) It is known^{10,19} that in the case of plane-wave phonons $R_{\text{LP}}(T) = \kappa_T M_{\text{Br}} - 1$, where κ_T is the isothermal compressibility, and M_{Br} is the adiabatic longitudinal modulus at the Brillouin line frequency. Using the relationships $v_0^2 \approx 1/\rho\kappa_T$ and $v_\infty^2 \approx M_\infty/\rho$, α can be expressed via the non-ergodicity parameter at T_g :

$$\alpha = (1 - f_0)/f_0 \quad (6)$$

$(1 - f_0)/f_0$ indeed correlates well with fragility¹⁰, as also does the non-ergodicity parameter f_0 . Substituting equation (5) into equation (6) gives $\alpha \propto K_\infty/G_\infty$. This provides a clear microscopic interpretation of the correlation between α and m reported in ref. 9: G_∞/K_∞ controls both the relative amplitude of the structural relaxation in a glass and the fragility of a supercooled liquid.

$f_0(T_g)$ also determines the amplitude of fluctuations frozen at T_g . That leads us to another unsolved problem—correlation between fragility and the amplitude of the boson peak²⁰. All disordered materials have an excess density of vibrational states, $g(\nu)$, over the Debye density of states, $g_{\text{Deb}}(\nu)$, in the terahertz frequency range^{20–24}, so that the ratio $g(\nu)/g_{\text{Deb}}(\nu)$ exhibits the so-called boson peak with amplitude A_{bp} . According to refs 20–25, A_{bp} is related to the amplitude of frozen structure fluctuations. So, one would expect higher A_{bp} in materials with higher $f_0(T_g)$ and thus A_{bp} should correlate with v_t/v_l and, consequently, with fragility. Comparison of $(v_t/v_l)^2$ and A_{bp} in a few glasses indeed shows very good correlation (Supplementary Fig. 1). Thus, the correlation of the boson peak amplitude to fragility observed in ref. 20 seems to be related to the same role of the non-ergodicity parameter. In other words, the capability of a structure to resist shear rather than bulk deformation also determines the boson peak amplitude through the amplitude of frozen fluctuations, $f_0(T_g)$.

Recently it was shown that higher anharmonicity of a glass-former corresponds to higher fragility^{8,11,26}. To understand this, we note that anharmonicity always leads to an increase of the fast relaxation in glasses²⁶, and thus, to a decrease of f_0 . Because, as we showed above, f_0 correlates with fragility, the same should be valid

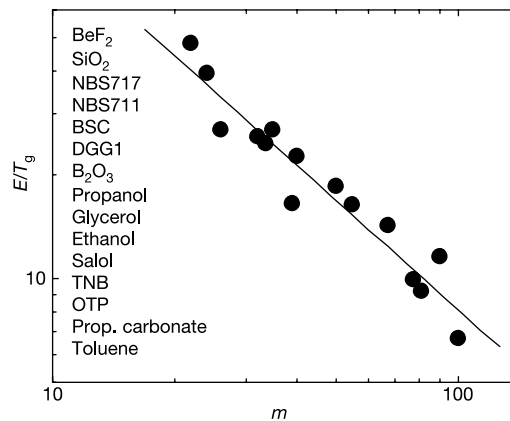


Figure 3 Correlation between fragility and the ratio of the high-temperature activation energy to the glass transition temperature. Materials are listed in ascending fragility order, where NBS717 is borosilicate glass, NBS711 is lead silica glass, BSC is borosilicate crown glass, TNB is 1,3,5-tri- α -naphthyl benzene and prop. is propylene. Data from the literature for fragility, the high-temperature slope of the fragility plot, E/T_g , and the respective references are given in Supplementary Table 1.

for the anharmonicity. A similar explanation can be applied to the correlation between the intensity of the fast relaxation normalized to the boson peak and the fragility found in ref. 8. The amplitude of the fast relaxation is related to $1 - f_0$, so the ratio of the fast relaxation to the boson peak should be proportional to $(1 - f_0)/f_0$, and correlate linearly with α and m .

Thus the ratio of instantaneous shear to bulk modulus in glasses, or, alternatively, the Poisson ratio, appears to be an important parameter that controls the fragility of liquids. This ratio also determines the non-ergodicity parameter f_0 , that is, how limited is the motion of a molecular unit in a cage formed by its neighbours. The same non-ergodicity parameter controls behaviour of the fast dynamics and that explains the correlation between fragility and fast dynamics in glass-forming systems. □

Received 1 June; accepted 17 August 2004; doi:10.1038/nature02947.

1. Anderson, P. W. Through a glass lightly. *Science* **267**, 1615 (1995).
2. Angell, C. A. Formation of glasses from liquids and biopolymers. *Science* **267**, 1924–1935 (1995).
3. Debenedetti, P. G. & Stillinger, F. H. Supercooled liquids and the glass transition. *Nature* **410**, 259–267 (2001).
4. Fox, K. C. Putting proteins under glass. *Science* **267**, 1922–1923 (1995).
5. Nemilov, S. V. The kinetics of elementary processes in the condensed state. II. Shear relaxation and the equation of state for solids. *Zh. Fiz. Khim.* **42**, 1391–1396 (1968); *Russ. J. Phys. Chem.* **42**, 726–731 (1968).
6. Nemilov, S. V. *Thermodynamic and kinetic aspects of the vitreous state* (CRC Press, Boca Raton, 1995).
7. Angell, C. A. Spectroscopy simulation and scattering, and the medium range order problem in glass. *J. Non-Cryst. Solids* **73**, 1–17 (1985).
8. Sokolov, A. P., Rössler, E., Kisliuk, A. & Quitmann, D. Dynamics of strong and fragile glassformers: differences and correlation with low-temperature properties. *Phys. Rev. Lett.* **71**, 2062–2065 (1993).
9. Scopigno, T., Ruocco, G., Sette, F. & Monaco, G. Is the fragility of a liquid embedded in the properties of its glass? *Science* **302**, 849–852 (2003).
10. Buchenau, U. & Wischniewski, A. Fragility and compressibility at the glass transition. Preprint at <http://arXiv.org/cond-mat/0401088> (2004).
11. Bordat, P., Affouard, F., Descamps, M. & Ngai, K. L. Does the interaction potential determine both the fragility of a liquid and the vibrational properties of its glassy state? Preprint at <http://arXiv.org/cond-mat/0401117> (2004).
12. Roland, C. M. & Casalini, R. Temperature dependence of local segmental motion in polystyrene and its variation with molecular weight. *J. Chem. Phys.* **119**, 1838–1842 (2003).
13. Barrer, R. M. The viscosity of pure liquids. I. Non-polymerised fluids. *Trans. Faraday Soc.* **39**, 48–59 (1943).
14. Stöckel, F., Fischer, E. W. & Richert, R. Dynamics of glass-forming liquids. II. Detailed comparison of dielectric relaxation, dc-conductivity, and viscosity data. *J. Chem. Phys.* **104**, 2043–2055 (1996).
15. Tobolsky, A., Powell, R. E. & Eyring, H. In *Frontiers in Chemistry* (eds Burk, R. E. & Grummit, O.) Vol. 1, 125 (Interscience, New York, 1943).
16. Dyre, J. C. & Olsen, N. B. Landscape equivalent of the shoving model. *Phys. Rev. E* **69**, 042501–042504 (2004).
17. Wang, W. H., Wen, P., Zhao, D. Q., Pan, M. X. & Wang, R. J. Relationship between glass transition temperature and Debye temperature in bulk metallic glasses. *J. Mater. Res.* **18**, 2747–2751 (2003).
18. Sanditov, D. S., Sangadiev, S. Sh. & Kozlov, G. V. On the correlation between elastic modulus of vitreous solids and glass transition temperature of melts. *Glass Phys. Chem.* **24**, 539–547 (1998).
19. Fabelinsky, I. L. *Molecular Scattering of Light* Ch. VII (Plenum, New York, 1968).
20. Sokolov, A. P. et al. Low-temperature anomalies in strong and fragile glass formers. *Phys. Rev. Lett.* **78**, 2405–2408 (1997).
21. Courtens, E., Foret, M., Hehlen, B. & Vacher, R. The vibrational modes of glasses. *Solid State Commun.* **117**, 187–200 (2001).
22. Grigera, T. S., Martin-Mayor, V., Parisi, G. & Verrocchio, P. Phonon interpretation of the 'boson peak' in supercooled liquids. *Nature* **422**, 289–292 (2003).
23. Malinovsky, V. K. & Sokolov, A. P. The nature of boson peak in Raman spectra in glasses. *Solid State Comm.* **57**, 757–761 (1986).
24. Duval, E., Boukenter, A. & Achibat, T. Vibrational dynamics and the structure of glasses. *J. Phys. Condens. Matter* **2**, 10227–10234 (1990).
25. Soltwisch, M., Quitmann, D. & Ruocco, G. On the connection between low frequency vibrational and relaxational motion in glasses. *J. Non-Cryst. Solids* **203**, 12–18 (1996).
26. Novikov, V. N. Vibration anharmonicity and fast relaxation in the region of glass transition. *Phys. Rev. B* **58**, 8367–8378 (1998).
27. Martinez, L.-M. & Angell, C. A. A thermodynamic connection to the fragility of glass-forming liquids. *Nature* **410**, 663–667 (2001).
28. Rössler, E., Hess, K.-U. & Novikov, V. N. Universal representation of viscosity in glass forming liquids. *J. Non-Cryst. Solids* **223**, 207–222 (1998).

Supplementary Information accompanies the paper on www.nature.com/nature.

Acknowledgements This work was supported by NSF and REFI grants.

Competing interests statement The authors declare that they have no competing financial interests.

Correspondence and requests for materials should be addressed to A.P.S. (alexey@uakron.edu).

Low-voltage organic transistors with an amorphous molecular gate dielectric

Marcus Halik¹, Hagen Klauk¹, Ute Zschieschang¹, Günter Schmid¹, Christine Dehm¹, Markus Schütz², Steffen Maisch², Franz Effenberger², Markus Brunnbauer³ & Francesco Stellacci³

¹Infineon Technologies AG, New Memory Platforms, Materials and Technology, Paul-Gossen-Straße 100, 91052 Erlangen, Germany

²University Stuttgart, Department of Chemistry, Pfaffenwaldring 55, 70569 Stuttgart, Germany

³Massachusetts Institute of Technology, Department of Materials Science and Engineering, 77 Massachusetts Avenue, Cambridge, Massachusetts 02139, USA

Organic thin film transistors (TFTs) are of interest for a variety of large-area electronic applications, such as displays^{1–3}, sensors^{4,5} and electronic barcodes^{6–8}. One of the key problems with existing organic TFTs is their large operating voltage, which often exceeds 20 V. This is due to poor capacitive coupling through relatively thick gate dielectric layers: these dielectrics are usually either inorganic oxides or nitrides^{2–8}, or insulating polymers⁹, and are often thicker than 100 nm to minimize gate leakage currents. Here we demonstrate a manufacturing process for TFTs with a 2.5-nm-thick molecular self-assembled monolayer (SAM) gate dielectric and a high-mobility organic semiconductor (pentacene). These TFTs operate with supply voltages of less than 2 V, yet have gate currents that are lower than those of advanced silicon field-effect transistors with SiO₂ dielectrics. These results should therefore increase the prospects of using organic TFTs in low-power applications (such as portable devices). Moreover, molecular SAMs may even be of interest for advanced silicon transistors where the continued reduction in dielectric thickness leads to ever greater gate leakage and power dissipation.

The use of SAM gate dielectrics for organic TFTs was pioneered by the Vuillaume group¹⁰. They investigated the mechanism of carrier tunnelling through SAMs and showed that current leakage through densely packed organic molecular monolayers with highly ordered aliphatic chains can be remarkably low, despite their thickness of only a few nanometres¹¹. To prepare organic TFTs (and even silicon metal–insulator–semiconductor field-effect transistors, MISFETs) with SAM dielectrics, the Vuillaume group relied on carboxyl-terminated *n*-alkyltrichlorosilanes^{10,12}. Using α -sexithiophene as the organic semiconductor, they demonstrated organic TFTs operating at 2 V, with a subthreshold swing of 350 mV per decade, a field-effect mobility of $3.6 \times 10^{-4} \text{ cm}^2 \text{ V}^{-1} \text{ s}^{-1}$, an on/off current ratio of 10^4 , and a gate current density of $10^{-6} \text{ A cm}^{-2}$ (ref. 10).

Given the small thickness of the molecular monolayers (about 2.5 nm), a gate current density of $10^{-6} \text{ A cm}^{-2}$ may seem reasonably low. However, the current density through a molecular monolayer can be less than $10^{-8} \text{ A cm}^{-2}$ (at 1 V) if no semiconductor is deposited¹¹. One possible explanation for the increase in gate current upon deposition of the organic semiconductor is the partial penetration of the SAM by the semiconductor molecules. This penetration is likely to reduce the dielectric thickness and create low-resistance current paths through the SAM. Such interaction between the SAM dielectric and the organic semiconductor is undesirable not only because it leads to increased gate leakage, but also because high-mobility carrier transport in the semiconductor depends critically on a well-defined semiconductor–dielectric interface.

To create dense self-assembled monolayers with sufficient robustness against molecular penetration, we have used a specifically